# University of California

# Ernest O. Lawrence Radiation Laboratory

## $K^+d$ INTERACTIONS NEAR 1 BeV/c

Allan A. Hirata, Charles G. Wohl, Roger W. Bland,
Gerson Goldhaber, Bronwyn H. Hall, John A. Kadyk,
Victor H. Seeger, and George H. Trilling

August 1968



Berkeley, California

## DISCLAIMER

Contribution to XIVth International
Conference on High-Energy Physics,
Vienna, August 28-September 5, 1968

UCRL-18322

UNIVERSITY OF CALIFORNIA

Lawrence Radiation Laboratory
Berkeley, California

AEC Contract No. W-7405-eng-48

# $K^+d$ INTERACTIONS NEAR 1 BeV/c

Allan A. Hirata, Charles G. Wohl, Roger W. Bland,
Gerson Goldhaber, Bronwyn H. Hall, John A. Kadyk,
Victor H. Seeger, and George H. Trilling

August 1968

# $K^+d$ INTERACTIONS NEAR 1 BeV/c*

Allan A. Hirata, Charles G. Wohl, Roger W. Bland,
Gerson Goldhaber, Bronwyn H. Hall, John A. Kadyk,
Victor H. Seeger, and George H. Trilling

Department of Physics and Lawrence Radiation Laboratory
University of California, Berkeley, California

## ABSTRACT

In this paper we present some detailed experimental results on the $K^+d$ interaction near 1 BeV/c. We give measurements on several inelastic cross sections and deduce the $I = 0$ inelastic cross section $KN\pi$. The latter corresponds largely to $K^*$ production and rises rapidly from 0.860 to 1.210 BeV/c. The results of a phase shift analysis of the charge-exchange data up to 0.860 BeV/c are also given. Furthermore we compare the charge-exchange data with a Regge model and find them to be consistent with the results of high-energy fits. So far we cannot give an unequivocal answer to the crucial question of whether or not a resonance occurs in the $I = 0$ KN system.

The $K^+p$ and $K^+d$ total cross sections, accurately measured by Cool et al.[1] and Bugg et al.,[2] have similarly-shaped asymmetric peaks near 1 BeV/c. The $K^+p$ cross section is the isospin-one KN cross section. The isospin-zero cross section is extracted from the $K^+p$ and $K^+d$ cross sections using approximations the validity and effect of which are not entirely known. The cross section so deduced has a large peak that might have been called a resonance were it in a $\pi N$ or $\bar{K}N$ channel. However the repercussions on classification schemes of the existence of KN resonances are severe. In particular, all well-established strongly-interacting particles and resonances have quantum numbers that permit their classification as quark-antiquark (meson) or triple-quark (baryon) states, and KN resonances will not fit into this scheme.

Bland et al.[3] studied $K^+p$ reactions around 1 BeV/c and found that the peak in the total cross section was due largely to the rapid increase of the single-pion-production cross section near the thresholds for the quasi-two-body channels $K\Delta(1236)$ and $K^*(890)N$. A partial-wave analysis of the reaction $K^+p \rightarrow K\Delta$ revealed no rapid variation of any of the phases. They concluded that there was no evidence requiring or even strongly suggesting a conventional single resonance in the $K^+p$ channel at 1.2 BeV/c.

In this paper we will discuss four aspects of the $K^+d$ interaction near 1 BeV/c. These represent various experimental results and some attempts at an analysis of the problem. So far we are not in a position to give an unequivocal answer to the central operation--whether or not a resonance occurs in the $I = 0$ $K^+N$ system. The subjects discussed are: A. A measurement of some of the partial $K^+d$ cross sections; B. Preliminary results on a phase shift analysis of the charge exchange reaction; C. Comparison of the charge exchange data with a Regge model; and D. Production and decay properties of some of the inelastic channels.

The results were obtained from a 100,000-picture exposure of the LRL 25-inch bubble chamber, filled with deuterium, to a separated $K^+$ beam at momenta of 863, 968, 1211, and 1364 MeV/c. The film was scanned twice for events with a vee ($K^o \to \pi^+\pi^-$ decay) or with more than two outgoing charged tracks. An event with an uneven number of outgoing charged tracks was either a $K^+$ decay or a $K^+d$ interaction in which the proton in the deuteron was spectator to an interaction on the neutron and did not have enough momentum to make a visible track. In the latter case, the absence of a track constitutes a measurement ipso facto, and in fitting we assigned to the unseen proton momentum zero with an uncertainty appropriate to a proton too slow to be visible. Events were measured on the LRL FSD or on a Franckenstein, and were processed with the programs SIOUX and ARROW. At these energies, events fitting more than one hypothesis could be resolved unambiguously by looking at track ionization. Failing events were remeasured until their number was reduced to an insignificant level. We found 3166 events with a $K^+$ and 5504 events with a $K^o$ in the final state. Cross sections were normalized with 2727 $K^+ \to \pi^+\pi^+\pi^-$ decays. In obtaining cross sections, $K^o$ events were weighted for decay into neutrals or outside the bubble chamber or too close to the production vertex for the vee to be seen as such.

## A. A Measurement of Some of the Partial $K^+d$ Cross Sections

We have measured some of the $K^+d$ partial cross sections around 1 BeV/c (Fig. 1), and calculate most of the others using relations derived from isospin conservation and data from the experiments mentioned above (Fig. 2). We also extract isospin-zero partial cross sections (Fig. 3). These lead to more understanding of the nature of this channel but are not sufficient to confirm or deny the existence of a resonance.

Cross sections directly measured. — The reactions that occur at these energies are:

$$
\begin{array}{llllll}
K^+d \rightarrow & KNN \rightarrow & K^+pn & & & \\
 & & \rightarrow K^0pp & & & * \\
 & \rightarrow KNN\pi \rightarrow & K^+nn\pi^+ & \left.\right\} & \sigma_c & \\
 & & \rightarrow K^0pn\pi^+ & & & * \\
 & & \rightarrow K^+pp\pi^- & & & * \\
 & & \rightarrow K^+pn\pi^0 & \left.\right\} & \sigma_o & \\
 & & \rightarrow K^0pp\pi^0 & & & * \\
 & \rightarrow KNN\pi\pi \rightarrow & K^0nn\pi^+\pi^+ & \left.\right\} & \sigma_{cc} & * \\
 & & \rightarrow K^+pn\pi^+\pi^- & & & * \\
 & & \rightarrow K^0pp\pi^+\pi^- & & & * \\
 & & \rightarrow K^+nn\pi^+\pi^0 & \left.\right\} & \sigma_{co} & \\
 & & \rightarrow K^0pn\pi^+\pi^0 & & & * \\
 & & \rightarrow K^+pp\pi^-\pi^0 & & & * \\
 & & \rightarrow K^+pn\pi^0\pi^0 & \left.\right\} & \sigma_{oo} & \\
 & & \rightarrow K^0pp\pi^0\pi^0 & & & *
\end{array}
\qquad (1)
$$

Reactions in which some of the final-state particles form particles or resonances (e.g., d, $K^*$, $N^*$) are not listed separately. We measured cross sections for the reactions marked to the right with an asterisk. The reactions are arranged according to the charge states of the pions, for reasons that will become clear. The symbol $\sigma_{co}$, for example, represents the sum of all cross sections leading to one charged and one neutral pion. Thus the total $K^+d \rightarrow KNN\pi\pi$ cross section is $(\sigma_{cc} + \sigma_{co} + \sigma_{oo})$, etc.

Figure 1(a) and Table I show the cross sections we measured. The $K^+d \rightarrow K^0pp$ cross section falls off smoothly with increasing momentum. The single-pion-production cross sections rise rapidly until about 1.2 BeV/c, then level off; they all have about the same shape, though they differ in size. The double-pion-production cross sections (only the sum of the measured cross sections is shown) are extremely small until 1.2 BeV/c, after which they begin to rise sharply. The thresholds for single and double pion production on deuterons are 0.45 and 0.70 BeV/c. (On free nucleons, the thresholds are 0.51 and 0.81 BeV/c.) The cross sections are small until well above the thresholds. In fact, they remain small until thresholds for $K^*$ and $N^*$ production are approached (see below).

Reactions such as $K^+d \to K^0pp$, $K^+d \to K^0pp\pi^0$, and $K^+d \to K^+pp\pi^-$, with two final-state protons, necessarily involve the neutron in the target deuteron as more than spectator. To the extent that one nucleon in the deuteron is only a spectator to the interaction of the incident $K^+$ with the other nucleon (an assumption we shall often make), these reactions take place on the neutron, and the cross sections give a somewhat distorted picture of free-neutron cross sections. In contrast, the $K^0pn\pi^+$ final state can come from interaction of the $K^+$ with either of the target nucleons (or from $K^+d \to K^0\pi^+d$). Figure 1(b) shows the division of the $K^+d \to K^0pn\pi^+$ cross section, with the spectator nucleon indicated by parentheses.[4] Also shown is the $K^+p \to K^0\pi^+p$ cross section measured by Bland.[3] The difference between the $K^+p \to K^0\pi^+p$ and $K^+p(n) \to K^0\pi^+p(n)$ cross sections is small and is consistent with a rough calculation of the effect of eclipsing and motion of the nucleons within the deuteron.

<u>Isospin conservation and $K^+d$ reactions</u>. — Isospin conservation provides one (and only one) linear relation between the $KNN\pi$ cross sections, and one between the $KNN\pi\pi$ cross sections. The relations are[5]:

$$\sigma_c = 2\sigma_o \tag{2a}$$

$$2\sigma_{cc} = 4\sigma_{oo} + \sigma_{co} \quad . \tag{2b}$$

We can now write the total $KNN\pi$ and $KNN\pi\pi$ cross sections in various ways, eliminating one or another of the constituent parts:

$$\sigma(KNN\pi) = \sigma_c + \sigma_o \tag{3a}$$
$$= 3\sigma_o \tag{3b}$$
$$= \frac{3}{2}\,\sigma_c \tag{3c}$$

$$\sigma(KNN\pi\pi) = \sigma_{cc} + \sigma_{co} + \sigma_{oo} \tag{4a}$$
$$= 3(\sigma_{cc} - \sigma_{oo}) \tag{4b}$$
$$= \frac{3}{2}\,(\sigma_{co} + 2\sigma_{oo}) \tag{4c}$$
$$= \frac{3}{4}\,(\sigma_{co} + 2\sigma_{cc}) \quad . \tag{4d}$$

We have not measured all of either $\sigma_c$ or $\sigma_o$ [see Eqs. (1)], nor all of any two of $\sigma_{cc}$, $\sigma_{co}$, and $\sigma_{oo}$. However this does not much restrict the usefulness of Eqs. (3) and (4) for obtaining $\sigma(KNN\pi)$ and $\sigma(KNN\pi\pi)$.

To complete $\sigma_c$ we need the $K^+d \rightarrow K^+nn\pi^+$ cross section. Here if the incident $K^+$ interacts with only one of the nucleons in the deuteron, it interacts with the proton. In view of the comparison made in Fig. 1(b) we may expect the approximation

$$\sigma(K^+d \rightarrow K^+nn\pi^+) \cong \sigma(K^+p \rightarrow K^+\pi^+n) \tag{5}$$

to be good to 10 or 20%. The $K^+p \rightarrow K^+\pi^+n$ cross section has been measured by Bland.[3] It is small, being never more than one-tenth the sum of the other, directly-measured parts of $\sigma_c$. Since the latter is measured to about 5%, Eq. (5) would have to be wrong by 50% to affect the value of $\sigma_c$ obtained using it by as much as a standard deviation. Small corrections to the approximation are inconsequential, especially since we double the quoted errors on $\sigma(K^+p \rightarrow K^+\pi^+n)$. Thus with Eq. (5) we complete $\sigma_c$, and with Eq. (3c) obtain $\sigma(KNN\pi)$.

Equations (4) for $\sigma(KNN\pi\pi)$ become inequalities if we put on the right just the parts of $\sigma_{cc}$, $\sigma_{co}$, and $\sigma_{oo}$ that are measured. Since all of $\sigma_{cc}$ is measured, Eq. (4b) gives an upper limit to $\sigma(KNN\pi\pi)$. The other three inequalities give lower limits, from which we may choose whichever is most restrictive. We then assign to $\sigma(KNN\pi\pi)$ the value midway between upper and lower limits, and fold together half the difference between the limits and the statistical uncertainty on them for an error.

Finally, subtracting the pion-production cross sections from the total cross section gives the $K^+d \to KNN$ cross section. Subtracting the $K^+d \to K^0pp$ cross section from this gives the $K^+d \to K^+pn$ cross section (this includes $K^+d \to K^+d$). Figure 2 and Table II show the results. Also shown are the total cross-section measurements of Cool et al.[1] and Bugg et al.[2] and $K^+d \to K^0pp$ measurements of Slater et al.[6] and Butterworth et al.[7] The most striking feature is the abrupt rise of the single-pion-production cross section to 15 mb at 1.2 BeV/c. As this is accompanied by a less precipitous fall of the KNN cross section, the total cross section increases by only about 10 mb. The onset of double pion production, by which time the single-pion-production cross section has leveled off, causes no marked change of the total cross section.

<u>Isospin conservation and $K^+N$ reactions</u>. — There are seven charge states for single pion production in $K^+N$ reactions:

$$\left.\begin{aligned} K^+p &\to K^0\pi^+p \\ &\to K^+\pi^+n \\ &\to K^+\pi^0p \end{aligned}\right\}\sigma_p \qquad \left.\begin{aligned} K^+n &\to K^0\pi^+n \\ &\to K^0\pi^0p \\ &\to K^+\pi^0n \\ &\to K^+\pi^-p \end{aligned}\right\}\sigma_n \qquad (6)$$

where $\sigma_p$ and $\sigma_n$ are the sums of the $K^+p$ and $K^+n$ cross sections. There are eleven charge states for double pion production. Isospin conservation provides one linear relation between the $KN\pi$ cross sections and one between the $KN\pi\pi$ cross sections. The relations are again Eqs. (2), in which the symbols now refer to a different set of reactions but are defined, as before, in terms of the charge states of the pions.

The cross sections for single pion production through the isospin-zero and -one channels are

$$\sigma_1(KN\pi) = \sigma_p \tag{7a}$$

$$\sigma_0(KN\pi) = 2\sigma_n - \sigma_p \quad . \tag{7b}$$

From Eqs. (7b) and (2a) one can obtain the relation

$$\sigma_0(KN\pi) = 3[\sigma(K^+n \to K^0\pi^+n) + \sigma(K^+n \to K^+\pi^-p) - \sigma(K^+p \to K^+\pi^0p)], \tag{8}$$

in which only three of the seven $KN \to KN\pi$ cross sections appear. The $K^+p \to K^+\pi^0p$ cross section has been measured by Bland.[3] The other two are approximately equal to the $K^+n(p) \to K^0\pi^+n(p)$ and $K^+d \to K^+pp\pi^-$ cross sections shown in Fig. 1. To get free-neutron cross sections from these, we have at each momentum multiplied them by the corresponding ratio of the $K^+p \to K^0\pi^+p$ to $K^+p(n) \to K^0\pi^+p(n)$ cross sections shown in Fig. 1(b). Although it is not strictly valid to apply to one channel the free-to-bound-nucleon cross-section ratios found in another, the errors on the ratios were probably large enough to encompass channel-to-channel variations, and they were propagated.[8] Figure 3 shows the values of $\sigma_0(KN\pi)$ we got. Also shown are total cross sections from Carter[9] and isospin-one partial cross sections adopted from a compilation made by Bland.[3] The smooth curve labeled $\sigma_0(KN\pi)$

was subtracted from $\sigma_0$(total) to get the elastic-scattering cross section $\sigma_0$(KN). We were not able to extract reliable values of $\sigma_0(KN\pi\pi)$, but even at 1364 MeV/c it is too small to do more than slightly reduce $\sigma_0$(KN).

Of $\sigma_0$(total) it must be said that at and below the peak the curves that appear in the literature are in only qualitative agreement. Below 1 BeV/c, even the purely statistical errors amount to one or two millibarns, and the elastic cross section is correspondingly uncertain. At low momenta, the total and elastic cross sections are equal, and their qualitative behavior is indicated by the low-momentum limit $\sigma = 4\pi A^2$, where A is the s-wave zero-effective-range scattering length. The lengths $A_0 = 0.04\pm0.04$ f.[10] and $A_1 = -0.30\pm0.01$ f.[11] give cross sections $\sigma_0 = 0.2^{+0.6}_{-0.2}$ mb and $\sigma_1 = 11.3\pm0.8$ mb. These strikingly dissimilar values make clear that $\sigma_0$(total), in contrast with $\sigma_1$(total), does in fact fall off rapidly at low momenta, as is indicated in Fig. 3.

The rapid increase of $\sigma_0(KN\pi)$ comes at the threshold for the quasi-two-body reaction $KN \rightarrow K^*N$. It appears to come at a slightly higher momentum than does the increase of $\sigma_1(KN\pi)$. This is reasonable, because the reaction $KN \rightarrow K\Delta$, for which the threshold is slightly lower and which is known to be the major part of $\sigma_1(KN\pi)$ in this region,[3] is forbidden to the isospin-zero channel. It is then surprising how similar in magnitude $\sigma_0(KN\pi)$ and $\sigma_1(KN\pi)$ quickly become. The rapid increase of $\sigma_0(KN\pi)$ combined with $\sigma_0$ total, where it must be remembered that the latter involves a number of approximations, results in a rapid decrease of $\sigma_0$(KN). Here it must be realized that $\sigma_0$(KN) carries the same approximation as $\sigma_0$ total. $\sigma_0$(KN) decreases more rapidly than does $\sigma_1$(KN), but no more than does the kinematic factor $4\pi\lambda\!\!\!^{-2}$, where $\lambda\!\!\!^-$ is the reduced wave length in the KN center-of-mass system.

B. Preliminary Results on a Phase Shift Analysis of the Charge Exchange Reaction

We present herewith the preliminary results we obtained in extending the phase shift analyses of Slater et al.[6] and Stenger et al.[10] to higher momenta. In addition to our own data we have also used the charge exchange measurements and in particular compared with the polarization data of Ray et al.[12] at 0.60 BeV/c. This data indicates a preference for the "Yang type" $I = 0$ KN solution.

We have carried out a joint fit of the data at 0.60 BeV/c, 0.81 BeV/c and our new data at 0.86 BeV/c. This fit differs from the earlier work in that at 0.81 and 0.86 BeV/c we have used the two $I = 1$ $K^+p$ solutions as discussed by Bland et al.[13] in the accompanying paper, namely $A_I^-$ and $A_{III}^-$, rather than only a pure s wave. For each of these we find as in the earlier work[6,10] the familiar Yang-Fermi ambiguity yielding a total of four sets $\text{Yang}_I$, $\text{Fermi}_{III}$ and $\text{Yang}_{III}$, $\text{Fermi}_I$. Here again as in the $K^+p$ case[13] we have applied the continuity condition from one momentum to the next. We have ignored the $I = 0$ inelastic cross section at 0.86 BeV/c, and we have checked that when this effect is included (by setting the $I = 0$ $\eta$ values equal to the $I = 1$ $\eta$ values, which is an overestimate) no substantial changes occur in the phase shifts. As was noted in the earlier work[6,10] a phase shift analysis on the charge exchange cross section data, together with $I = 1$ phase shifts, can lead to a variety of solutions which differ considerably in $\sigma_0$, the $I = 0$ total cross section, and in the quasi elastic scattering cross section. For the present analysis we have used the values for $\sigma_0$ of Cool et al.[1] at 0.81 and 0.86 BeV/c with generous errors as an additional constraint in the fit. At a later date we hope to compare with experimental quasi elastic data. As mentioned above the charge exchange polarization data of Ray et al.[12] as well as the analysis of the $K^0p$ data of Kadyk et al.[14] by Kim[15] indicates that the

Yang solutions are strongly preferred. If we combine this with the polarization information from the $K^+p$ scattering[16] the $\mathrm{Yang}_I$ solution is singled out preferentially. At the moment we cannot rule out the possibility of the presence of other as yet undetected solutions. The four phase shift sets are listed in Table III and the two Yang sets are plotted in Fig. 4. Figure 5 shows the fits to $\frac{d\sigma}{d\Omega}$ C.E. for 0.86 BeV/c. Figure 6 shows the resulting charge exchange polarization for the two Yang sets. The polarization for the two Fermi sets look essentially the same except for a change in sign. The correspondence is between $\mathrm{Yang}_I$ and $\mathrm{Fermi}_{III}$ and between $\mathrm{Yang}_{III}$ and $\mathrm{Fermi}_I$. Figure 7 gives the differential cross section for quasi elastic scattering for the two Yang sets. With our constraint on $\sigma_o$ the qualitative appearance of the quasi elastic scattering is similar for all solutions quoted here, although some quantitative difference exists.

Here it is of course of interest to extend this analysis to the 0.860, 0.97, and 1.21 BeV/c data. Unfortunately in this region we do not as yet know how to distribute the $\eta$ values. Work on this question is currently in progress.

C. Comparison of the Charge-Exchange Reaction with a Regge Model

Rarita and Schwarzschild[17] successfully fitted the differential cross section for $K^+n \to K^0p$ at 2.23 BeV/c, as well as some other data involving charged t-channel exchanges, using the well-established ρ and $A_2$ poles and a less-well-established ρ' trajectory. We have used their formalism and their fitted parameters, with two slight modifications, to predict the properties of the KN charge-exchange reaction at momenta below 2.23 BeV/c. We find remarkable agreement with experiment even down to 0.97 BeV/c.

The two modifications we make have negligible effect at high energies but improve the agreement with the low-energy data. The first is a simple change in the formalism that increases its validity at low energies: in the usual high-energy approximation the laboratory beam energy E appears in the Regge amplitudes in the form $A \propto (E/E_0)^{\alpha}$, $B \propto (E/E_0)^{\alpha-1}$. In our calculations we replace E by the less approximate form $E + t/(4M_p)$. The correction term $t/(4M_p)$ is clearly negligible in either the high-energy or low-momentum-transfer limit. However the shape of the differential cross section below 2.23 BeV/c is appreciably affected. Our second modification is to vary the ρ' spin-flip residue function $D = D_0 e^{D_1 t}$ as follows: $D_0$ from − 264 to − 135 mb, and $D_1$ from 2.95 to 2.3 $(\text{GeV/c})^{-2}$. These changes somewhat decrease the quality of the fit at 2.23 BeV/c, but give good agreement with the lower-energy data down to 0.97 BeV/c.

Figure 8 shows the experimental charge-exchange cross section as a function of beam momentum, integrated from the forward direction to $t = -1\ (\text{BeV/c})^2$. (We regard the Regge model as unreliable for larger momentum transfers.) We have included our cross sections, that of Butterworth et al. at 2.23 BeV/c,[7] and those of Slater et al.[6] from threshold to 0.81 BeV/c. The dashed curve is the prediction using the unmodified Rarita-Schwarzschild result. The solid curve is the result after our modifications. Figure 9 shows the experimental differential cross sections from 2.23 to 0.97 BeV/c. The curves have the same meaning as in Fig. 8. While about 20% low at 2.23 BeV/c, the solid curves give a good representation of the data at the lower momenta.

While we have not performed a complete Regge fit to our charge exchange data, the calculation described here indicates that the Rarita-Schwarzschild fit could easily be extended to momenta spanning the structure in the $I = 0$ and $I = 1$ total KN cross sections near 1200 MeV/c. It is interesting to note that the Regge model appears to fit rather well at low momenta both the charge exchange and the $K^+p$ elastic scattering.[13]

D. Production and Decay Properties of Some of the Inelastic Channels

We are analyzing the production and decay angular distributions of the inelastic channels. The main feature here--as was the case for the $I = 1$ $K^+p$ interaction--is that the differential distributions at 1.2 BeV/c are very similar to those at higher momenta.[7,18] The $K^{*o}$ production has the characteristics of pion exchange in the t-channel, in contrast with $K^{*+}$ production which has the characteristics of $\omega$ and P' exchange. We illustrate these features with the 1.2-BeV/c $K^+d$ data. Figures 10 and 11 show the Dalitz plots for the reactions

$$K^+d \rightarrow K^+\pi^-p(p)$$

$$\text{and} \qquad K^+d \rightarrow K^o\pi^+p(n) \quad .$$

Figures 12 and 13 show the corresponding mass projections, production angular distribution $\theta(K^*)$ in the overall c.m. system, and the decay angular distributions for the polar angle $\alpha(K^*)$ and Treiman-Yang angle $\varphi(K^*)$ in the $K^*$ c.m. system.

As may be noted, the $\cos\theta(K^*)$ distribution is highly forward peaked for $K^{*o}$ production and much less so for $K^{*+}$ production. The $\cos\alpha(K^*)$ distribution has a considerable $\cos^2\alpha$ component for $K^{*o}$ and a strong $\sin^2\alpha$ component for $K^{*+}$. The $\varphi(K^*)$ distribution is nearly flat for $K^{*o}$ and has the features characteristic of vector exchange for $K^{*+}$. Here it must be noted that no cutoffs or corrections have been applied for the $\Delta(1236)$ band. Figure 13 also shows a comparison with the same reaction as observed in hydrogen. The agreement between the two, both expressed in percent, is remarkably good and serves as a test for our procedures.

Finally, Fig. 14 shows what we get for the $I = 0$ $K\pi$ and $p\pi$ mass and $K^*$ production angular distributions by applying relation (8) to the differential cross sections. As may be noted the $\Delta(1236)$ signal vanishes--as expected. Also the $I = 0$ $K^*$ differential cross section is strongly forward peaked, indicating the presence of several partial waves in the s-channel.

## NOTES AND REFERENCES

*Work supported by the U. S. Atomic Energy Commission.

1. R. L. Cool, G. Giacomelli, T. F. Kycia, B. A. Leontic, K. K. Li, A. Lundby, and J. Teiger, Phys. Rev. Letters 17, 102 (1966). We thank Dr. T. F. Kycia for sending us slightly revised results.

2. D. V. Bugg, R. S. Gilmore, K. M. Knight, D. C. Salter, G. H. Stafford, E. J. N. Wilson, J. D. Davies, J. D. Dowell, P. M. Hattersley, R. J. Homer, A. W. O'Dell, A. A. Carter, R. J. Tapper, and K. F. Riley, Phys. Rev. 168, 1466 (1968).

3. R. W. Bland, M. G. Bowler, J. L. Brown, G. Goldhaber, S. Goldhaber, V. H. Seeger, and G. H. Trilling, Phys. Rev. Letters 18, 1077 (1967). Final results and a more complete discussion may be found in R. W. Bland, Single Pion Production in the $K^+p$ Channel from 860 to 1360 MeV/c (Ph.D. Thesis), Lawrence Radiation Laboratory Report UCRL-18131 (March 1968).

4. The simplest way to make the division is to take the slower nucleon to be the spectator. This overestimates the smaller $[K^+n(p) \rightarrow K^0\pi^+n(p)]$ cross section and underestimates the larger. We have corrected for this effect.

5. There are three independent isospin amplitudes for the reactions $K^+d \rightarrow KNN\pi$ (and $K^+N \rightarrow KN\pi$), and six for the reactions $K^+d \rightarrow KNN\pi\pi$ (and $K^+N \rightarrow KN\pi\pi$). Equations (2) are independent of the relative importance of the amplitudes. It is a lengthy process to derive the relations using Clebsch-Gordan coefficients. A method given by Shmushkevich enables one to write them down almost at once. See I. Shmushkevich, Doklady Akad. Nauk SSSR 103, 235 (1955) [translated by M. Hamermesh, AEC-tr-2270]; N. Dushin and I. Shmushkevich, Soviet Physics Doklady 1, 94 (1956); G. Pinski, A. J. Macfarlane, and E. C. G. Sudarshan, Phys. Rev. 140, B1045 (1965).

6. W. Slater, D. H. Stork, H. K. Ticho, W. Lee, W. Chinowsky, G. Goldhaber, S. Goldhaber, and T. O'Halloran, Phys. Rev. Letters 7, 378 (1961).

7. I. Butterworth, J. L. Brown, G. Goldhaber, S. Goldhaber, A. A. Hirata, J. A. Kadyk, B. M. Schwarzschild, and G. H. Trilling, Phys. Rev. Letters 15, 734 (1965), as well as additional unpublished results.

8. From low to high momentum, the ratios are 1.14±0.14, 1.28±0.11, 1.07±0.06, and 1.12±0.10. Within errors the ratios are almost constant, although the $K^+p \rightarrow K^0\pi^+p$ cross section more than quadruples.

9. A. A. Carter, The Argand Diagrams of the KN and $\bar{K}$N Forward Scattering Amplitudes, Cavendish Laboratory Report HEP 68-10 (March 1968). A dispersion-relation calculation using all the latest available data, including those from refs. 1 and 2.

10. V. J. Stenger, W. E. Slater, D. H. Stork, H. K. Ticho, G. Goldhaber, and S. Goldhaber, Phys. Rev. 134, B1111 (1964).

11. S. Goldhaber, W. Chinowsky, G. Goldhaber, W. Lee, T. O'Halloran, T. F. Stubbs, G. M. Pjerrou, D. H. Stork, and H. K. Ticho, Phys. Rev. Letters 9, 135 (1962).

12. A. K. Ray, R. W. Burris, H. E. Fisk, R. W. Kraemer, D. G. Hill, and M. Sakitt, APS Meeting, Washington, April 1968, and H. E. Fisk, private communication.

13. R. W. Bland, G. Goldhaber, B. H. Hall, J. A. Kadyk, V. H. Seeger, G. H. Trilling, and C. G. Wohl, $K^+p$ Interactions Near 1 BeV/c, Contribution to XIVth International Conference on High-Energy Physics, Vienna, 1968, UCRL-18323.

14. J. A. Kadyk, Y. Oren, G. Goldhaber, S. Goldhaber, G. H. Trilling, Phys. Rev. Letters 17, 599 (1966).

15. J. K. Kim, Phys. Rev. Letters 19, 1074 (1967).

16. S. Femino, S. Jannelli, F. Mezzanares, L. Monari, and P. Serra, Nuovo Cimento 50A, 371 (1967).

17. W. Rarita and B. Schwarzschild, Phys. Rev. 162, 1378 (1967).

18. G. Bassompierre et al., Contribution to the Heidelberg International Conference on Elementary Particles, CERN/D.Ph.II/Physics 67-19.

Table I. $K^+d$ scattering cross sections (in mb).

| | Channel | Momentum (MeV/c) 863 | 968 | 1211 | 1364 |
|---|---|---|---|---|---|
| Cross sections directly measured | $K^+d \to K^0pp$ | 6.72±0.40 | 6.26±0.29 | 4.99±0.24 | 3.69±0.29 |
| | $\to K^0pp\pi^0$ | 0.48±0.08 | 0.82±0.08 | 2.09±0.13 | 2.06±0.19 |
| | $\to K^0pn\pi^+$ | 1.24±0.14 | 2.47±0.16 | 6.21±0.29 | 6.08±0.42 |
| | $\to K^+pp\pi^-$ | 0.46±0.05 | 0.91±0.05 | 2.89±0.12 | 3.21±0.20 |
| | $\to KNN\pi\pi$[a] | --- | 0.01±0.005 | 0.11±0.02 | 0.59±0.07 |
| Components of $K^+d \to K^0pn\pi^+$ | $K^+d \to K^0\pi^+d$ | 0.13±0.04 | 0.13±0.03 | 0.14±0.03 | 0.18±0.05 |
| | $K^+p(n) \to K^0\pi^+p(n)$ | 0.98±0.13 | 1.99±0.15 | 4.76±0.26 | 4.78±0.38 |
| | $K^+n(p) \to K^0\pi^+n(p)$ | 0.13±0.04 | 0.35±0.05 | 1.31±0.12 | 1.12±0.15 |
| Derived cross sections[b] | $K^+d \to KNN$ | 27.59±0.32 | 27.17±0.35 | 22.73±0.63 | 20.97±0.99 |
| | $\to K^+pn$ | 20.87±0.56 | 20.91±0.50 | 17.74±0.78 | 17.28±1.15 |
| | $\to KNN\pi$ | 2.74±0.24 | 5.54±0.29 | 14.51±0.60 | 15.54±0.95 |
| | $\to KNN\pi\pi$ | --- | 0.01±0.005 | 0.17±0.05 | 0.76±0.18 |
| | $K^+d$ total[c] | 30.33±0.21 | 32.72±0.19 | 37.41±0.20 | 37.27±0.15 |

[a] This is the sum over the six (of eight) charge channels observed.

[b] These include cross sections for the reactions in which NN is a deuteron.

[c] From Bugg et al.

Table II. Isospin-zero KN scattering cross sections (in mb).

| Channel[a] | Momentum (MeV/c) 863 | 968 | 1211 | 1364 |
|---|---|---|---|---|
| KN → all[b] | 22.5 | 24.0 | 24.1 | 21.9 |
| KN → KN | 21.5 | 21.5 | 16.1 | 13.0 |
| KN → KNπ | 1.0±0.4 | 2.5±0.6 | 8.0±1.0 | 8.9±1.8 |

[a]We were not able to extract KN → KNππ cross sections, but even at 1364 MeV/c it is much smaller than the errors on the other cross sections.

[b]From Carter. Errors are unknown but sizable.

Table III. Phase shifts for fit at 0.60, 0.81, 0.86 BeV/c.

| | $Yang_I$ solution | | | $Yang_{III}$ solution | | |
|---|---|---|---|---|---|---|
| Momentum (BeV/c) | 0.60 | 0.81 | 0.86 | 0.60 | 0.81 | 0.86 |
| $\delta_{S_{1/2}}$ | 7.7±0.6 | 13±2.8 | 18±8.0 | 7.5±0.6 | 14±4.2 | 18±6.3 |
| $\delta_{P_{1/2}}$ | 24.4±1.8 | 29±4.3 | 34±5.9 | 22.9±1.7 | 23±4.5 | 21±6.6 |
| $\delta_{P_{3/2}}$ | 4.7±0.6 | 15±2.5 | 19±4.9 | 5.0±0.6 | 3.8±2.1 | 4.6±2.9 |
| $\delta_{D_{3/2}}$ | -13.3±1.4 | -16±3.1 | -20±4.8 | -14.3±1.3 | -26±2.7 | -33±5.0 |
| $\delta_{D_{5/2}}$ | 1.9±0.4 | 0.0±2.0 | 0.8±2.5 | 2.2±0.4 | 7±2.0 | 7±2.4 |
| $\chi^2$ | 12.5 | 3.0 | 18.7 | 12.9 | 2.7 | 22.7 |
| Degrees of freedom | 5 | 3 | 15 | 5 | 3 | 15 |
| $\sigma_{tot}$ (I=0) (mb) | 12.4 | 14.1 | 19.2 | 12.4 | 16.0 | 19.2 |
| | $Fermi_I$ solution | | | $Fermi_{III}$ solution | | |
| Momentum (BeV/c) | 0.60 | 0.81 | 0.86 | 0.60 | 0.81 | 0.86 |
| $\delta_{S_{1/2}}$ | 7.5±0.6 | 13±4.2 | 17±9.2 | 8.2±0.6 | 13±3.1 | 18±7.7 |
| $\delta_{P_{1/2}}$ | 0.1±1.1 | -2.5±2.4 | -2.8±3.2 | -0.7±1.3 | 6±4.5 | 6±6.0 |
| $\delta_{P_{3/2}}$ | 16.5±1.0 | 17±4.1 | 14±4.9 | 17.2±1.0 | 26±2.7 | 33±3.4 |
| $\delta_{D_{3/2}}$ | 5.4±0.7 | 13±2.5 | 16±2.9 | 4.9±0.8 | 1.6±2.7 | 2.1±3.2 |
| $\delta_{D_{5/2}}$ | -11.0±0.8 | -20±2.2 | -25±2.2 | -10.4±1.0 | -9±3.2 | -9±4.6 |
| $\chi^2$ | 12.6 | 2.6 | 22.4 | 12.5 | 5.2 | 16.6 |
| Degrees of freedom | 5 | 3 | 15 | 5 | 3 | 15 |
| $\sigma_{tot}$ (I=0) (mb) | 12.2 | 16.6 | 19.6 | 12.2 | 12.5 | 17.5 |

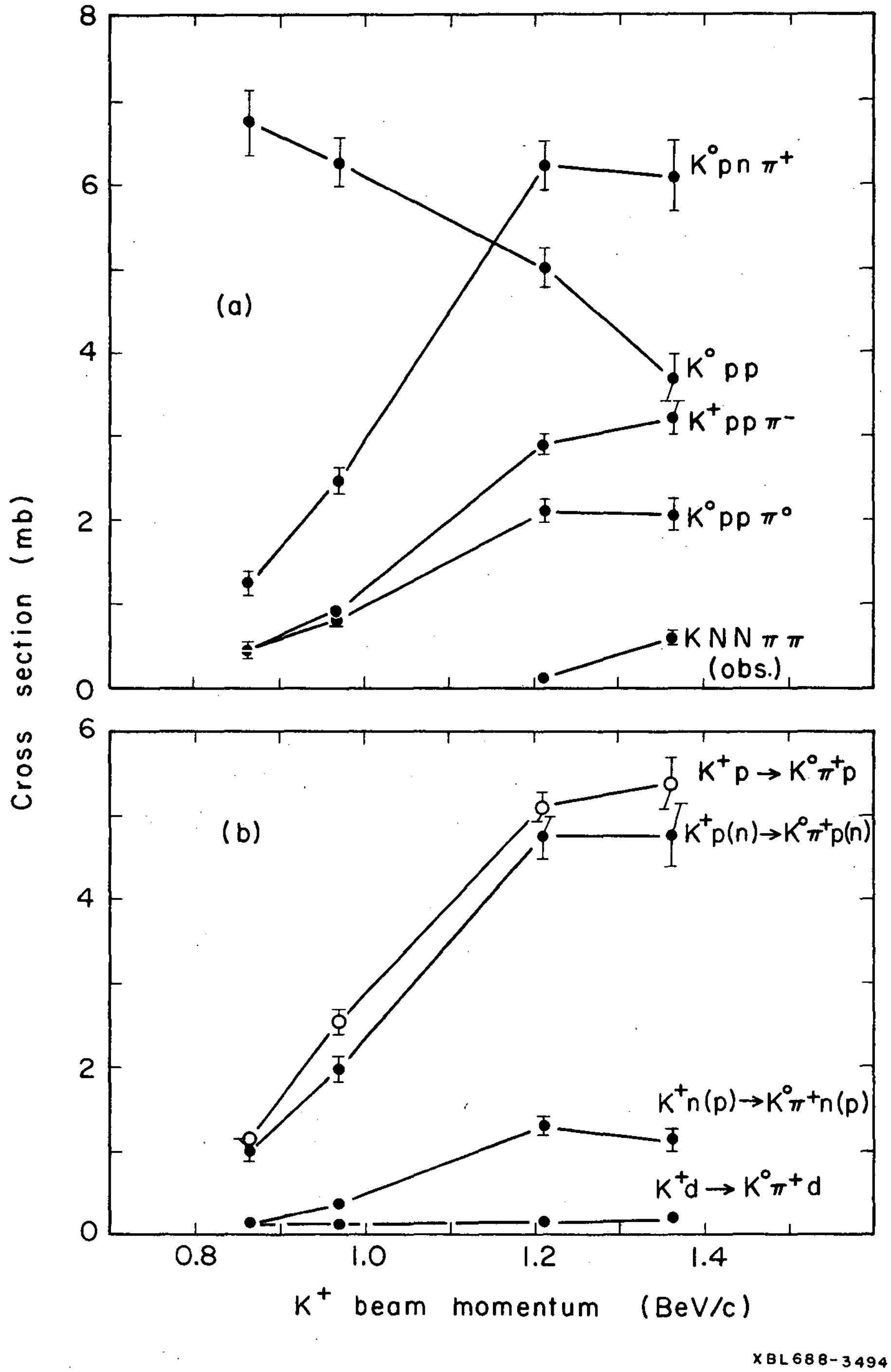


Fig. 1. (a) $K^+d$ partial cross sections measured in this experiment. (b) Components of the $K^+d \rightarrow K^o pn\pi^+$ cross section. Also shown is the $K^+p \rightarrow K^o\pi^+p$ cross section measured by Bland et al.[3]

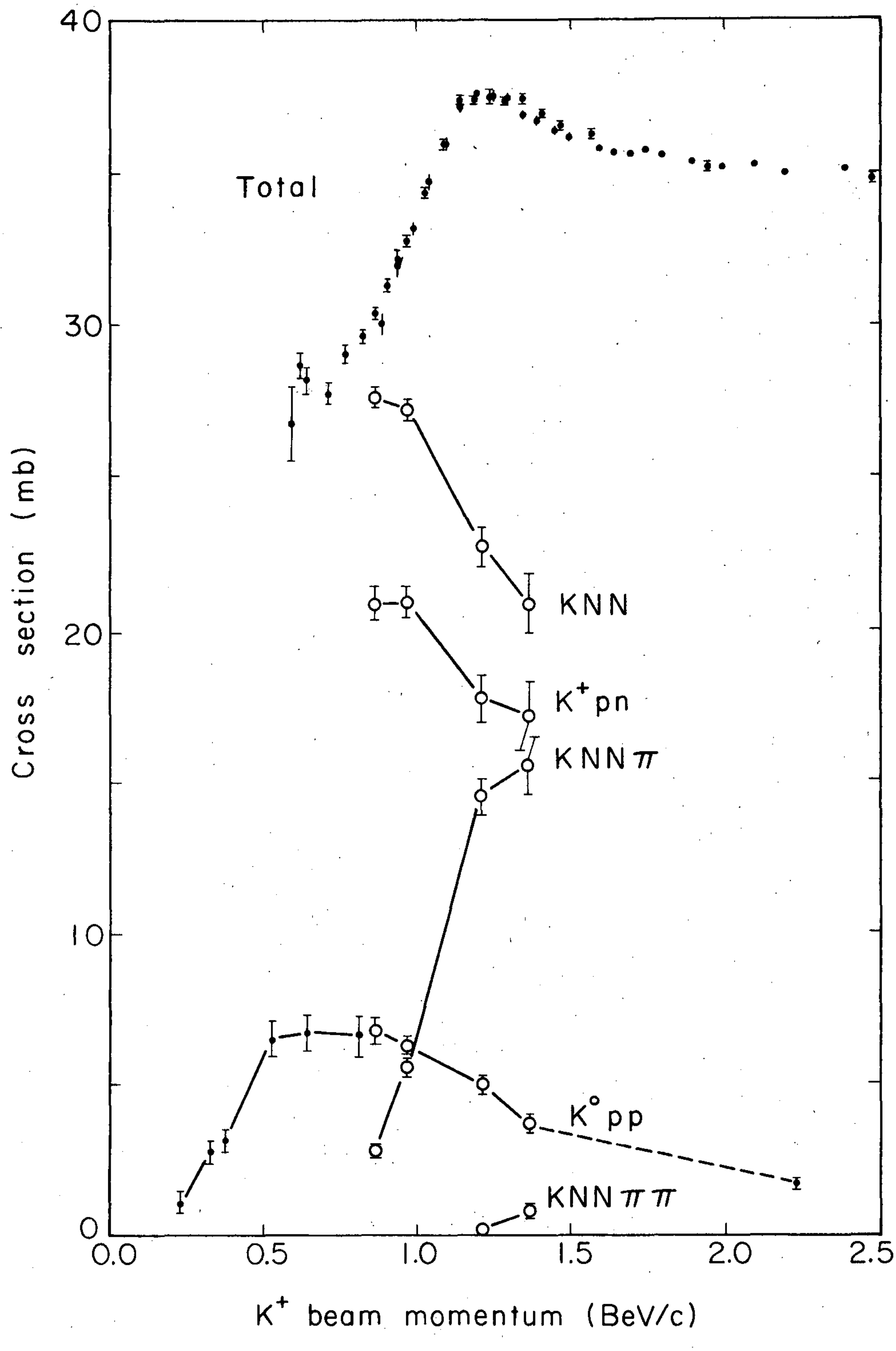


Fig. 2. $K^+d$ total and partial cross sections. Total cross sections are from Cool et al.[1] and Bugg et al.[2] The $K^+d \rightarrow K^opp$ cross sections at low momenta are from Slater et al.[6]; that at 2.3 BeV/c is from Butterworth et al.[7]

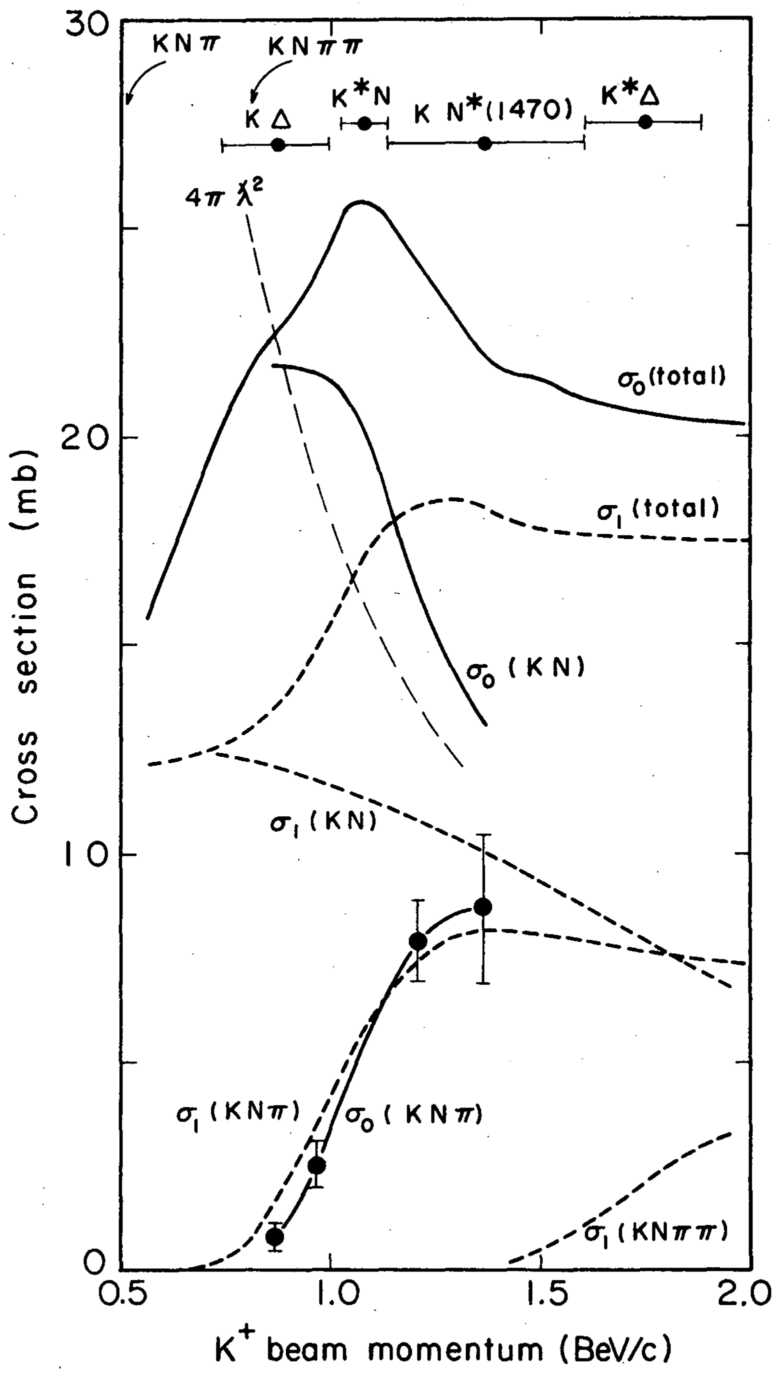


Fig. 3. Isospin-zero and -one cross sections. Total cross sections are from a compilation of all available data by Carter.[8] Here the isospin-zero total cross sections are deduced from the data of Cool et al.[1] and Bugg et al.[2] assuming folding and the Glauber-Wilkin correction. Isospin-one partial cross sections are adapted from the compilation of Bland et al.[3]

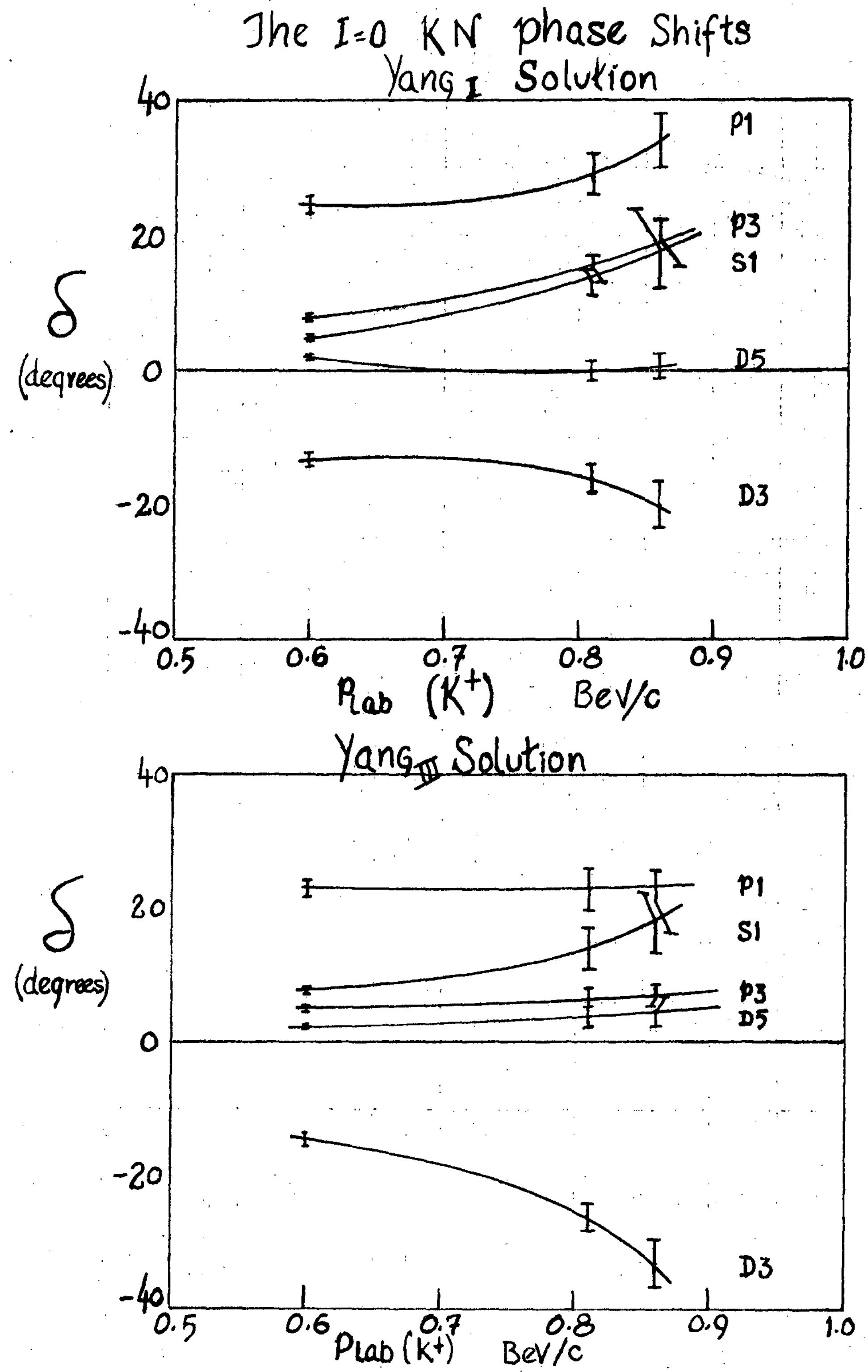
The I=0 KN phase Shifts
Yang I Solution
40
20
0
-20
-40
δ
(degrees)
P1
P3
S1
D5
D3
0.5
0.6
0.7
0.8
0.9
1.0
Plab (K+) BeV/c
Yang III Solution
40
20
0
-20
-40
δ
(degrees)
P1
S1
P3
D5
D3
0.5
0.6
0.7
0.8
0.9
1.0
Plab (K+) BeV/c

Fig. 4

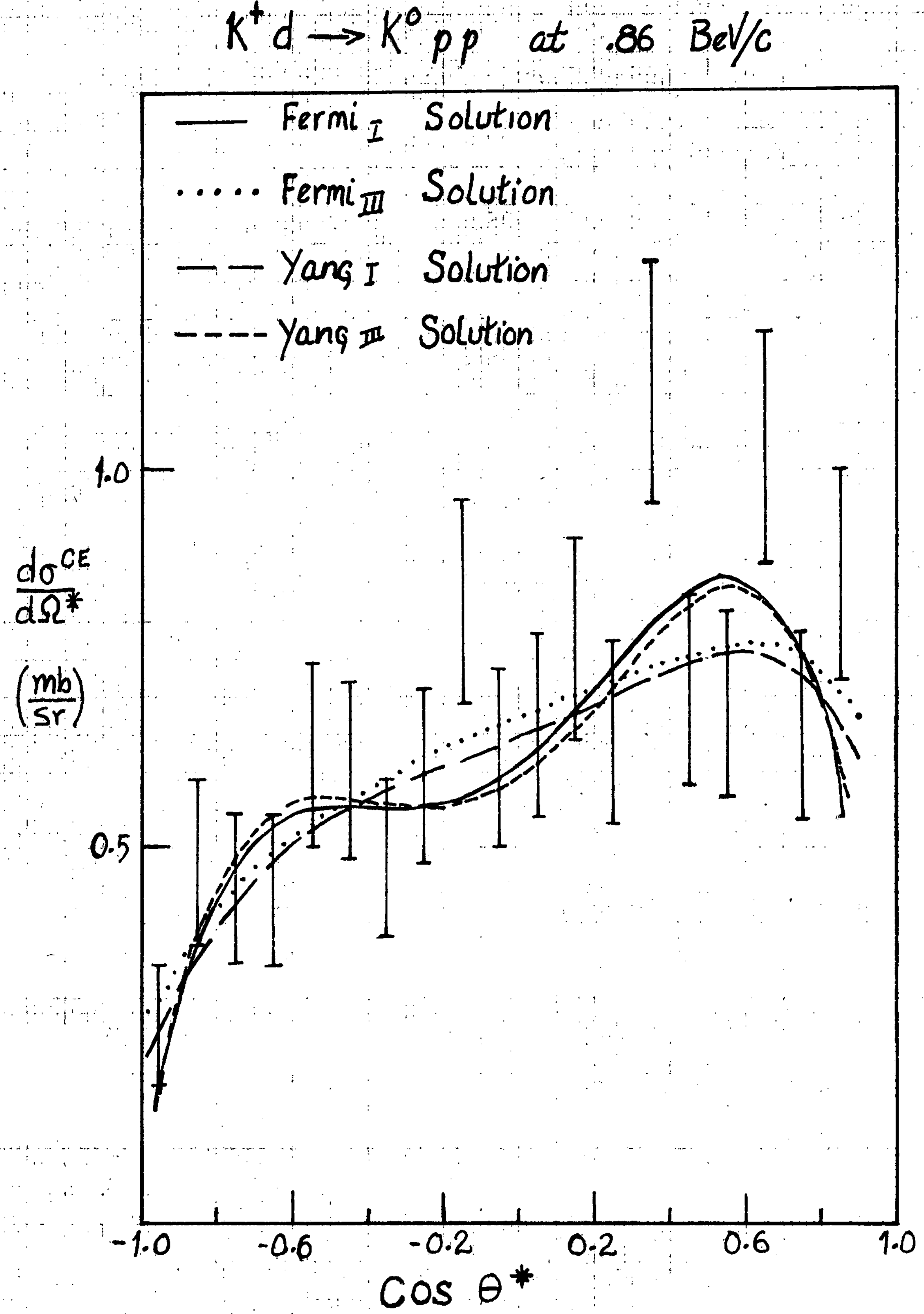
K+d → K0 p p at .86 BeV/c
Fermi I Solution
Fermi III Solution
Yang I Solution
Yang III Solution
1.0
0.5
dσCE/dΩ*
(mb/sr)
-1.0
-0.6
-0.2
0.2
0.6
1.0
Cos θ*

Fig. 5

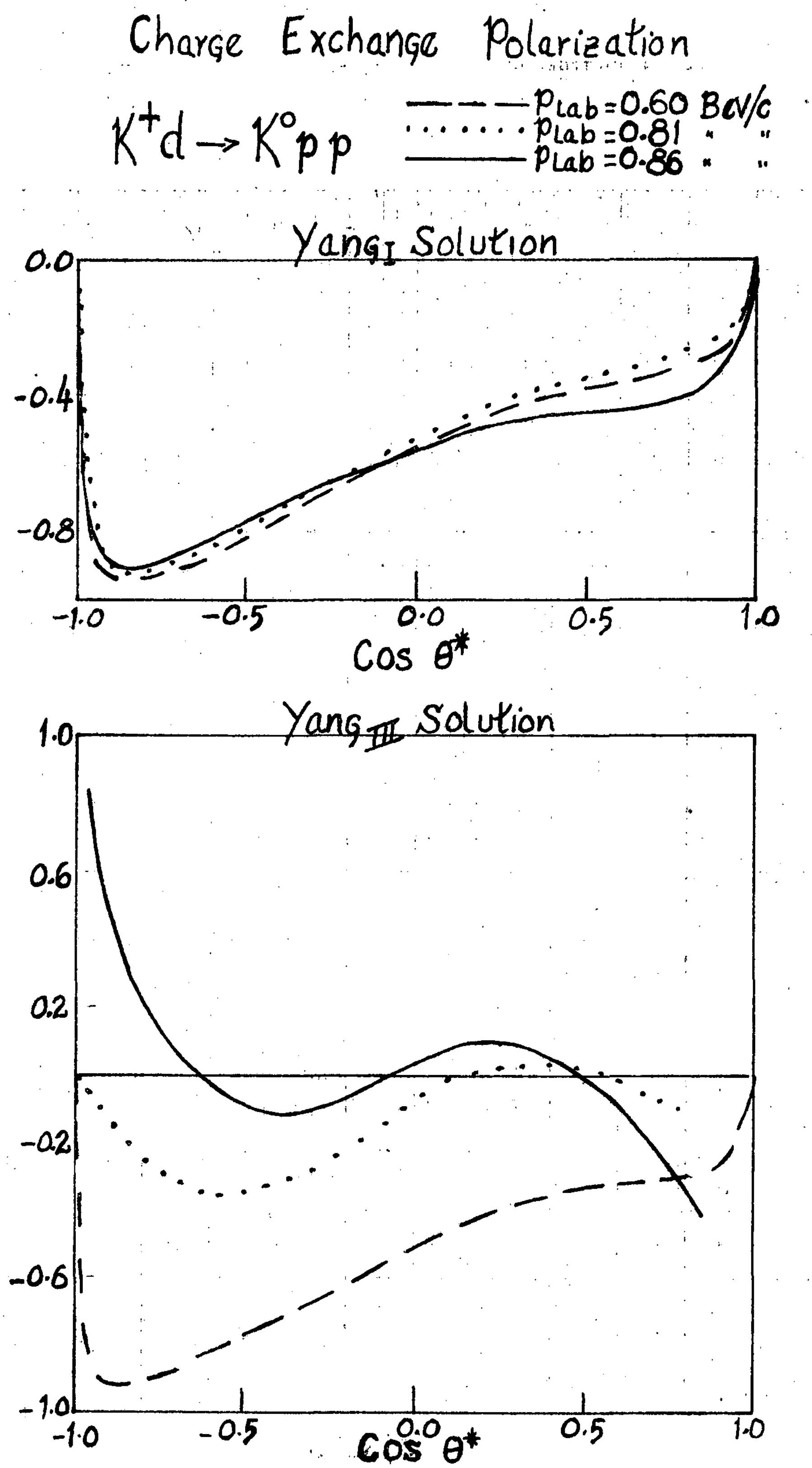
Charge Exchange Polarization
K+d → K°pp
plab = 0.60 BeV/c
plab = 0.81 " "
plab = 0.86 " "
Yang_I Solution
0.0
-0.4
-0.8
-1.0
-0.5
0.0
0.5
1.0
Cos θ*
Yang_III Solution
1.0
0.6
0.2
-0.2
-0.6
-1.0
-1.0
-0.5
0.0
0.5
1.0
Cos θ*

Fig. 6

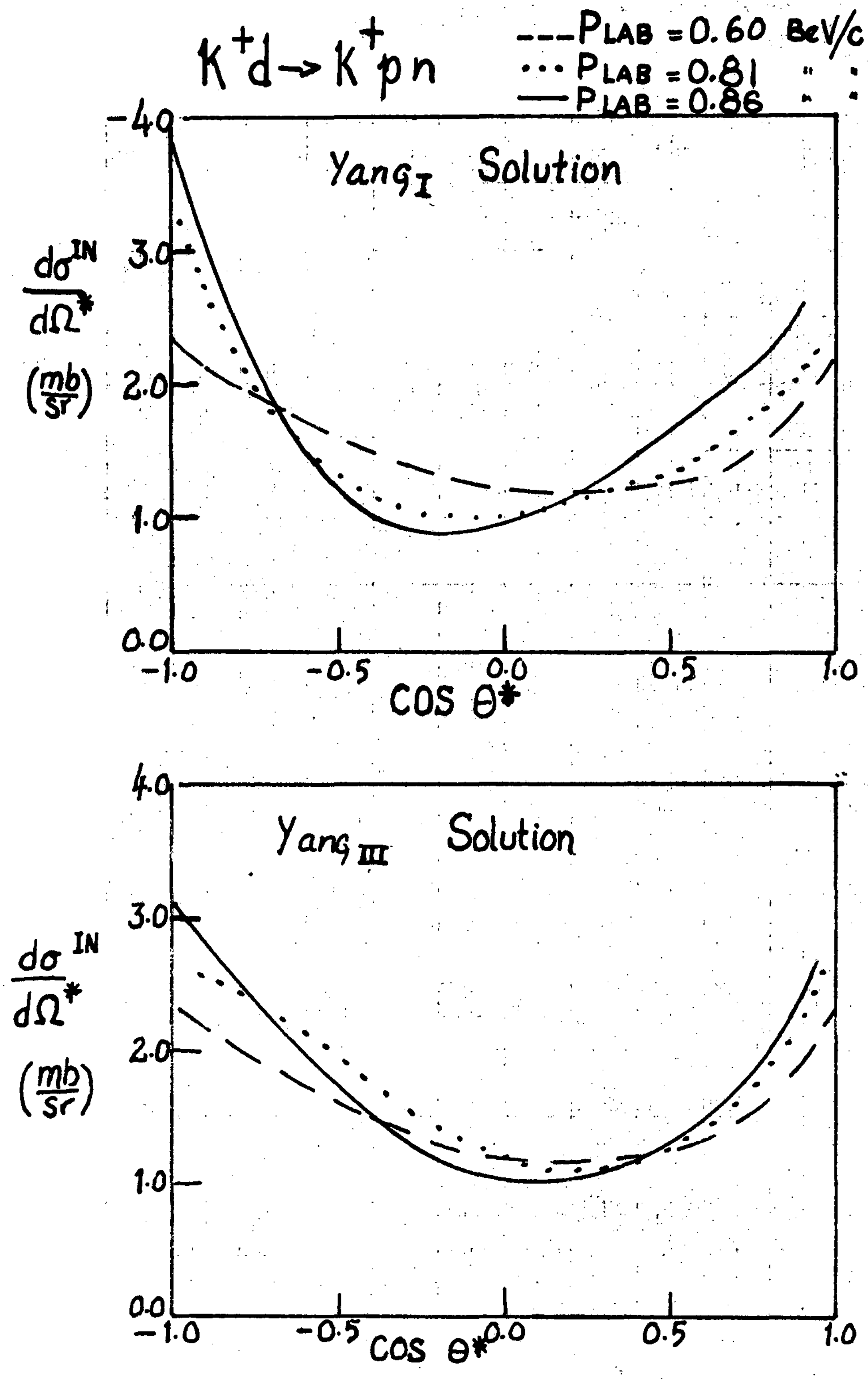
K+d → K+pn
---PLAB = 0.60 BeV/c
··· PLAB = 0.81 "
— PLAB = 0.86 "
Yang I Solution
dσ IN / dΩ*
(mb/Sr)
4.0
3.0
2.0
1.0
0.0
-1.0
-0.5
0.0
0.5
1.0
COS θ*
Yang III Solution
dσ IN / dΩ*
(mb/Sr)
4.0
3.0
2.0
1.0
0.0
-1.0
-0.5
COS θ*
0.0
0.5
1.0

Fig. 7

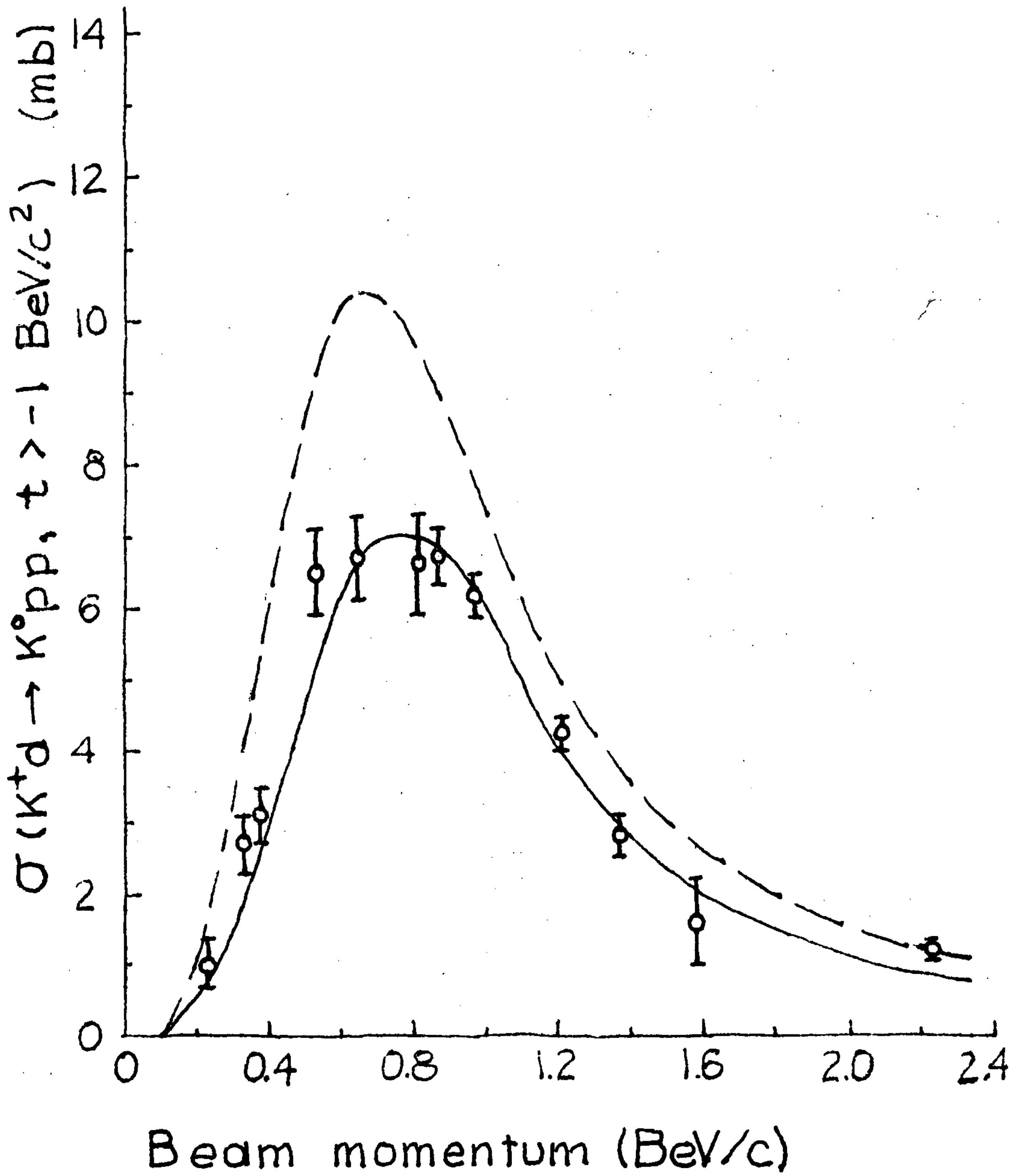


XBL 688-5658

Fig. 8

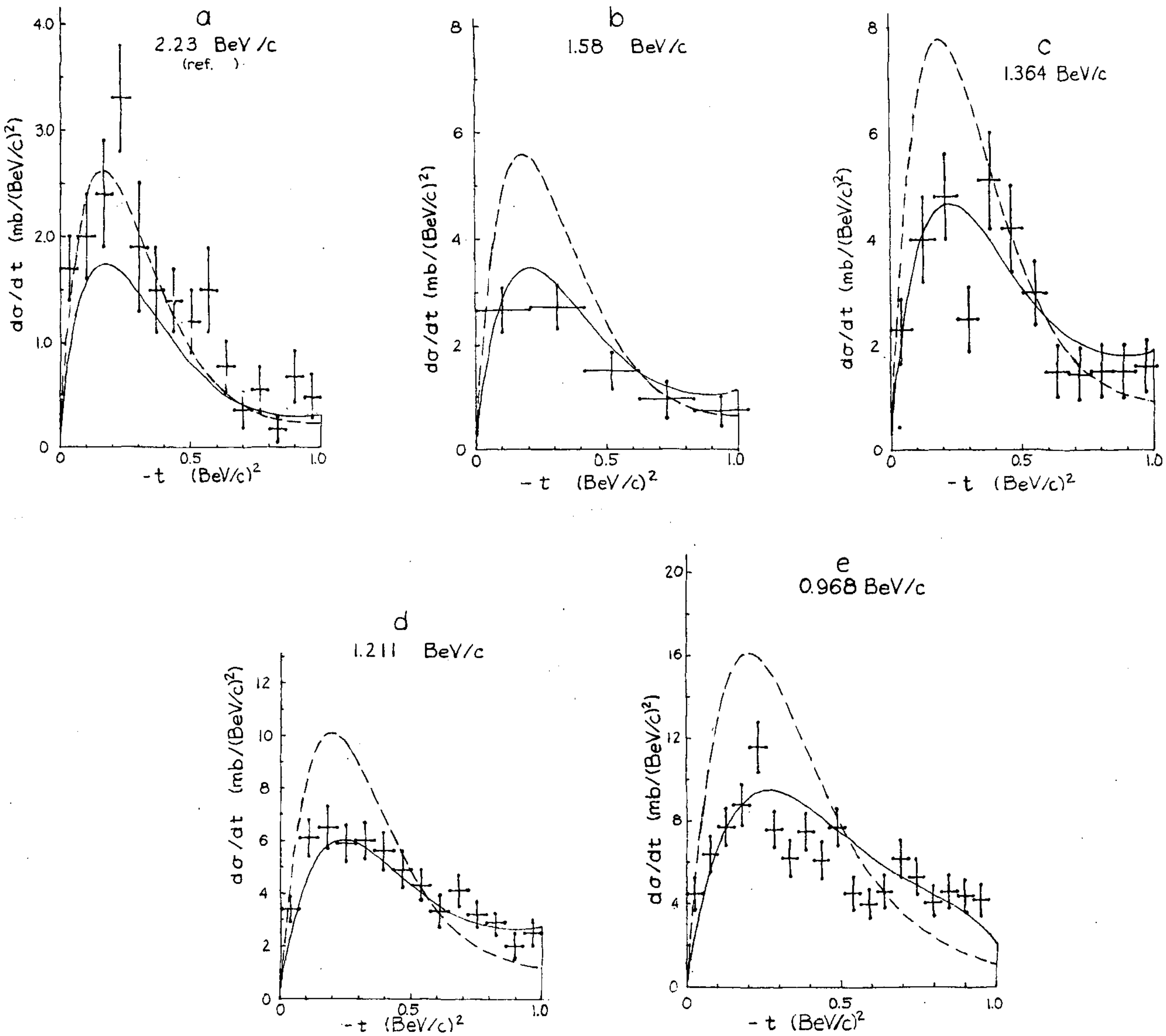
a
2.23 BeV/c
(ref. )
b
1.58 BeV/c
c
1.364 BeV/c
d
1.211 BeV/c
e
0.968 BeV/c
dσ/dt (mb/(BeV/c)²)
-t (BeV/c)²
XBL 688-5659

Fig. 9

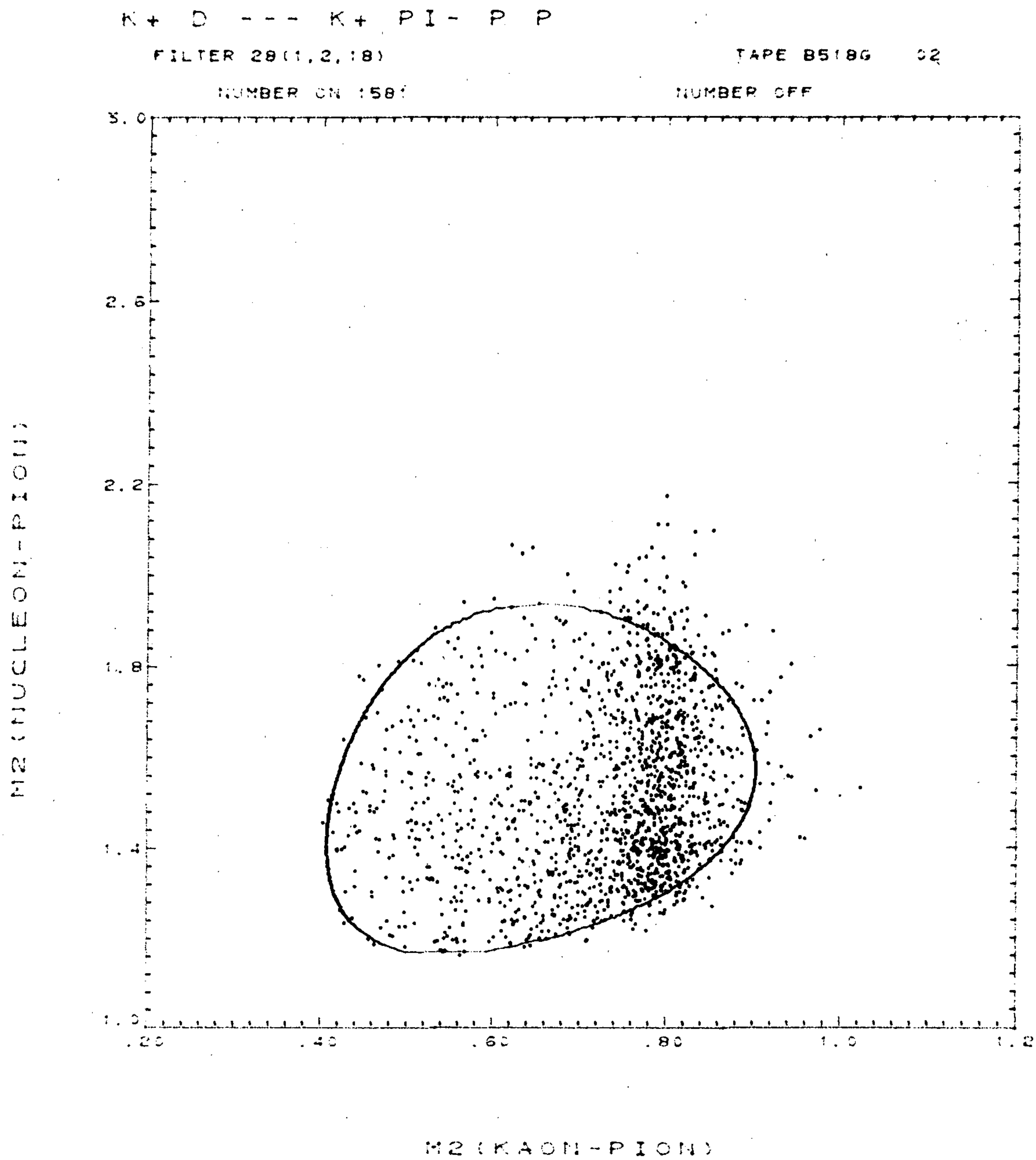


XBL 689-5966

Fig. 10

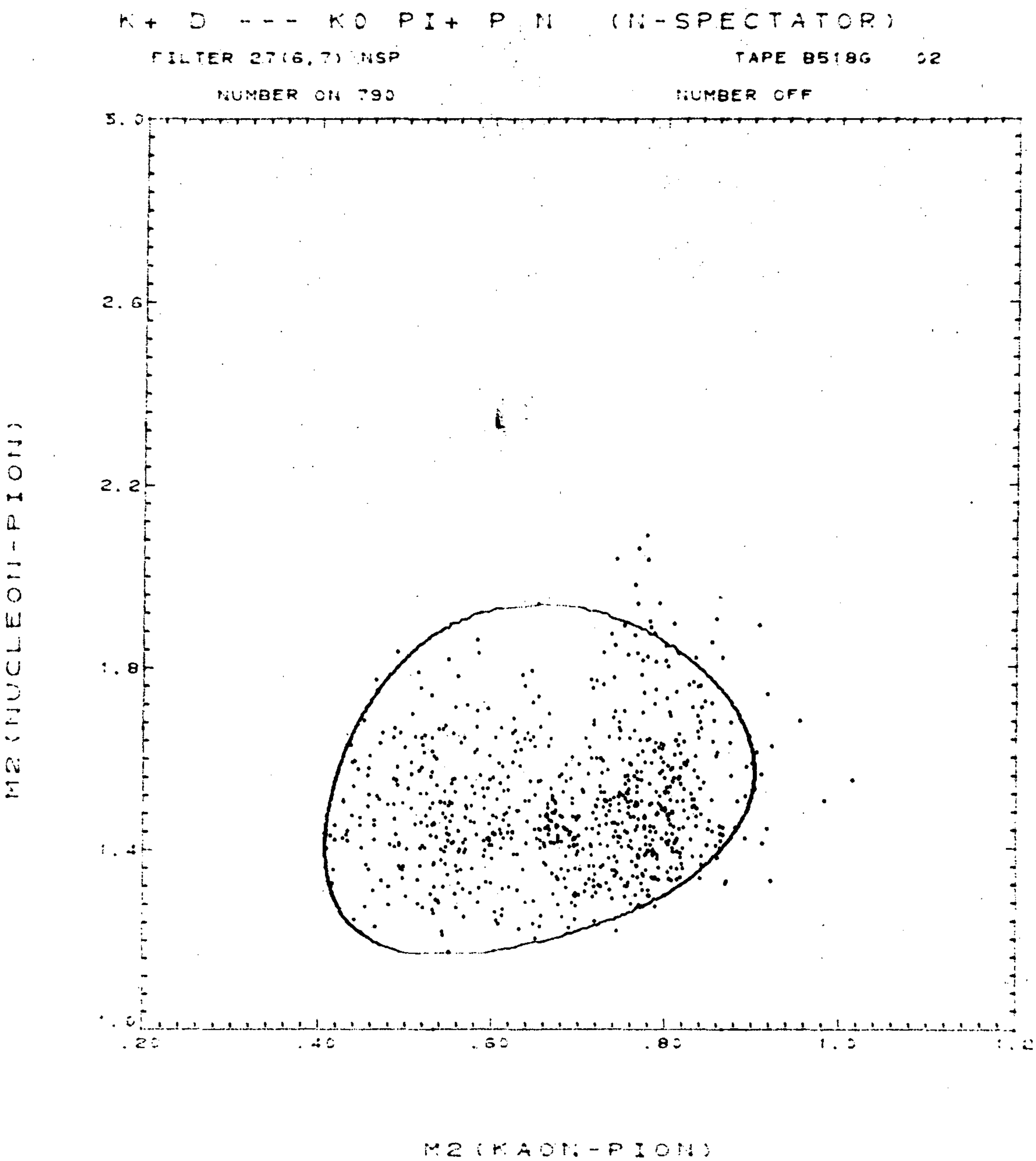


XBL 689-5967

Fig. 11

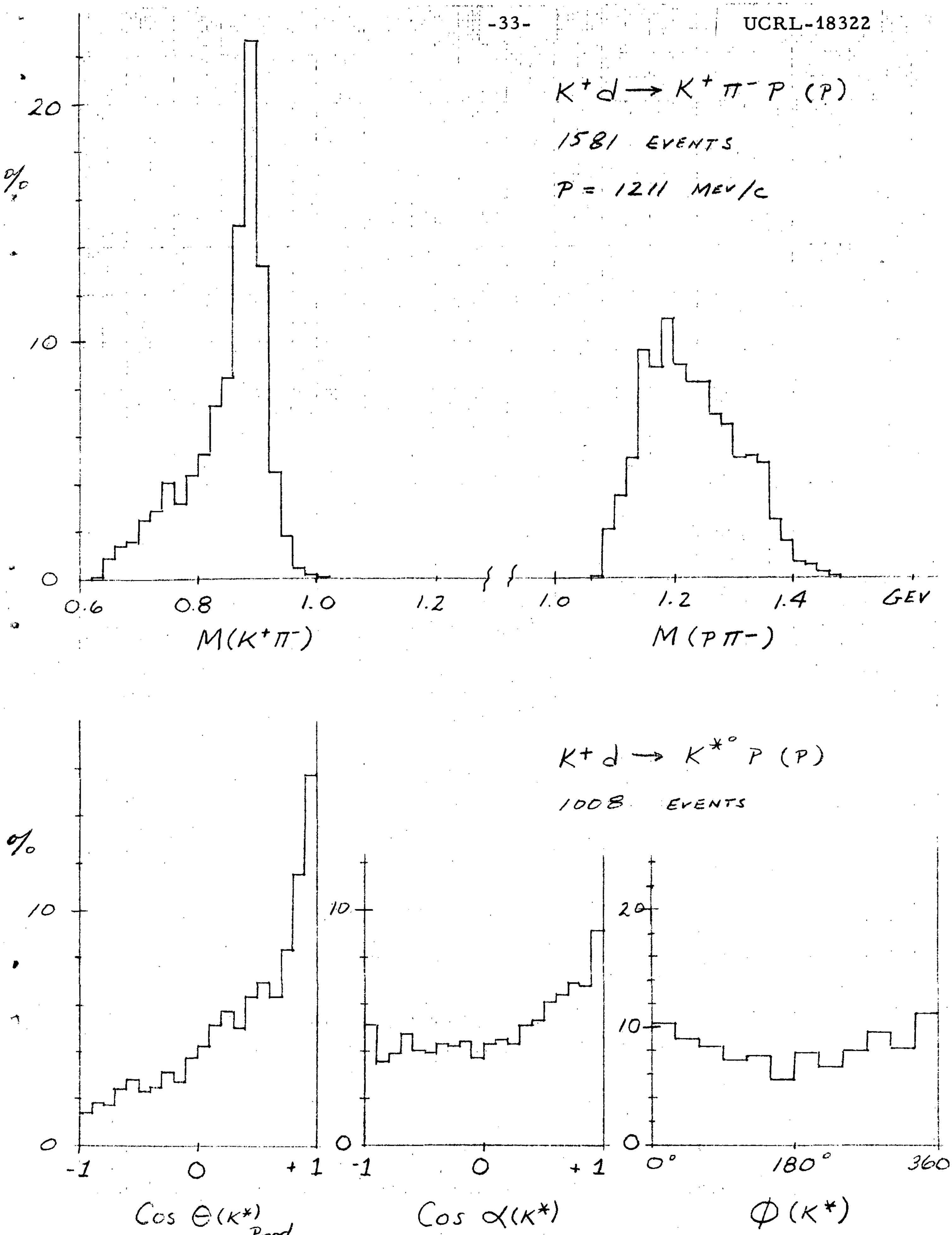

$K^+d \rightarrow K^+\pi^-p\ (p)$
1581 EVENTS
P = 1211 MEV/c
%
20
10
0
0.6
0.8
1.0
1.2
1.0
1.2
1.4
GEV
$M(K^+\pi^-)$
$M(p\pi^-)$
$K^+d \rightarrow K^{*0}p\ (p)$
1008 EVENTS
%
10
0
-1
0
+1
10
0
-1
0
+1
20
10
0
0°
180°
360°
$\cos\theta(K^*)_{Prod.}$
$\cos\alpha(K^*)$
$\phi(K^*)$


Fig. 12

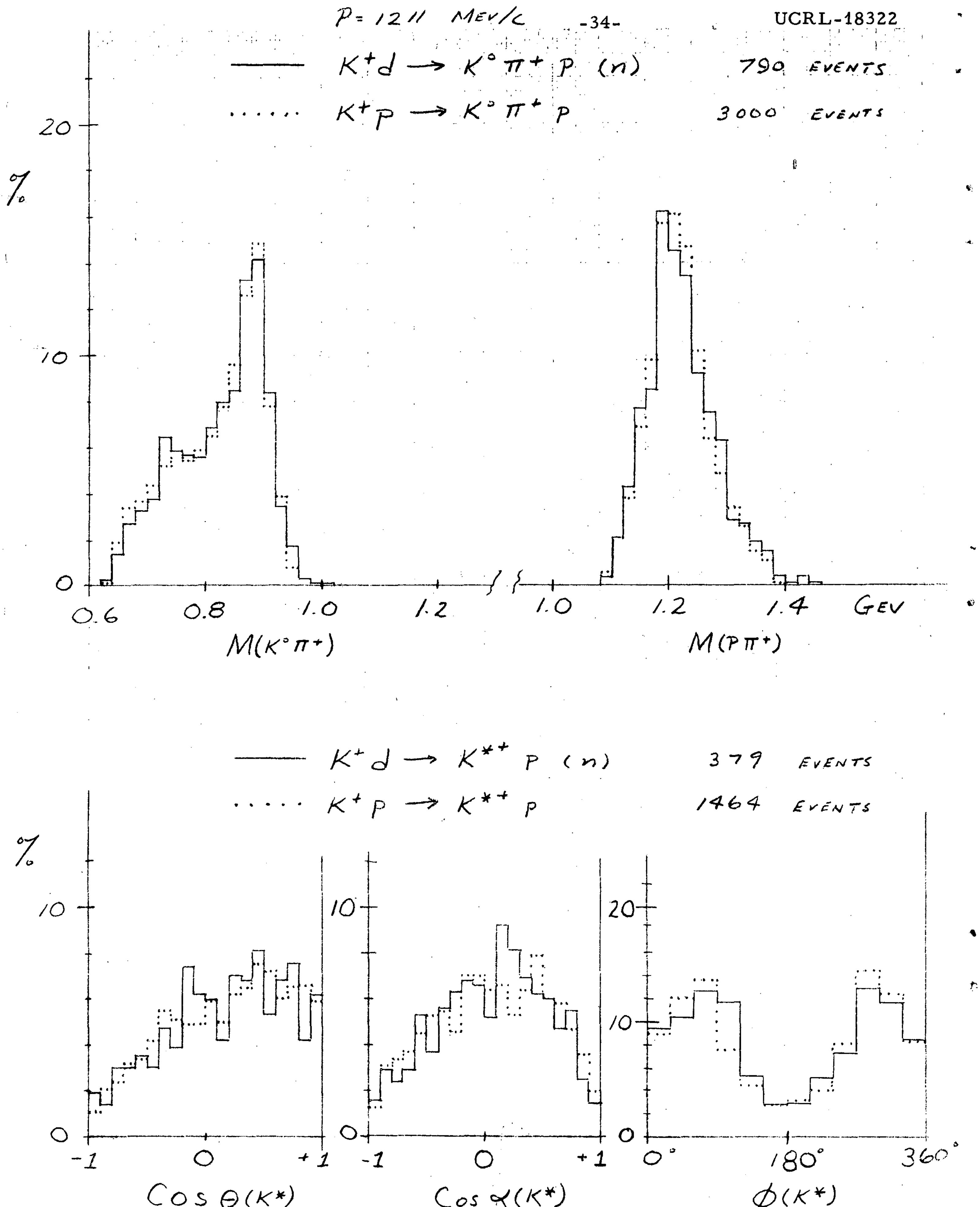
P = 1211 MEV/C
K⁺d → K°π⁺p (n) 790 EVENTS
K⁺p → K°π⁺p 3000 EVENTS
%
20
10
0
0.6
0.8
1.0
1.2
1.0
1.2
1.4
GEV
M(K°π⁺)
M(pπ⁺)
K⁺d → K*⁺p (n) 379 EVENTS
K⁺p → K*⁺p 1464 EVENTS
%
10
0
20
-1
0
+1
0°
180°
360°
Cos Θ(K*) Prod.
Cos α(K*)
φ(K*)

Fig. 13

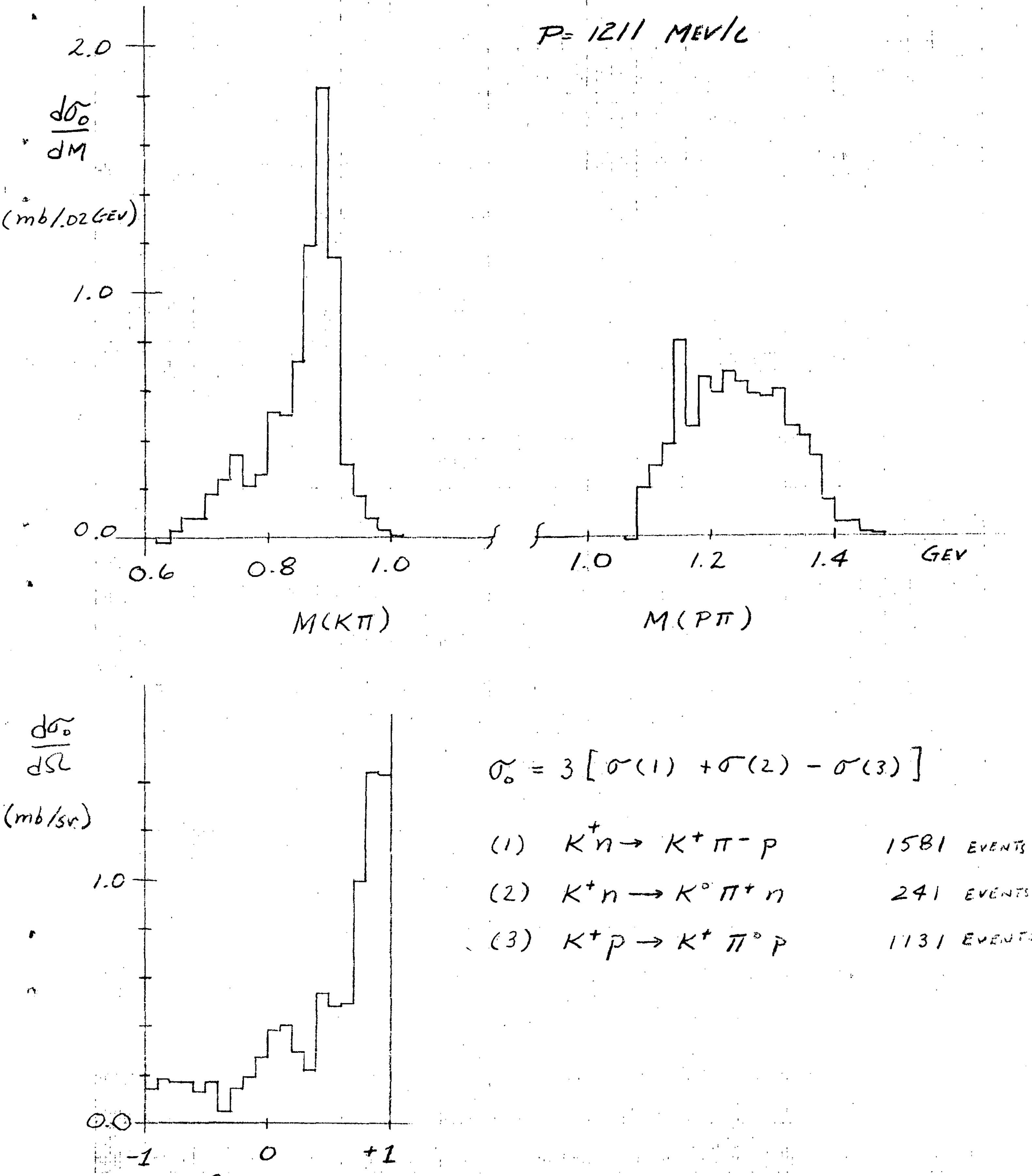
P = 1211 MEV/c
dσ₀/dM
(mb/.02 GEV)
2.0
1.0
0.0
0.6
0.8
1.0
M(Kπ)
1.0
1.2
1.4
GEV
M(Pπ)
dσ₀/dΩ
(mb/sr)
1.0
0.0
-1
0
+1
Cos Θ(K*) Prod.
σ₀ = 3 [σ(1) + σ(2) − σ(3)]
(1) K⁺n → K⁺π⁻p 1581 EVENTS
(2) K⁺n → K°π⁺n 241 EVENTS
(3) K⁺p → K⁺π°p 1131 EVENTS

Fig. 14